SPECTRAL INDEXING OF CHEMICAL WEATHERING IN THE MID-INFRARED: NEW MEANS TO EVALUATE WEATHERING ON MARS. M. D. Kraft[1], C. M. Alvarado[1], T. G. Sharp[1], and E. B. Rampe[1], [1]Arizona State University, School of Earth and Space Exploration, P.O. Box 1404, Tempe, AZ 85287-1404, United States; mdkraft@asu.edu.

Introduction: Spectroscopic observations offer the best means to evaluate chemical weathering on Mars at regional and global scales. Near-infrared (NIR) spectral data from OMEGA and CRISM have revealed hydrated minerals that indicate aqueous alteration, including different clay minerals [1-3], sulfates [1,4], silica [5], and carbonates [6], which are regionally localized across the Martian highlands. Mid-infrared (MIR) spectra from TES have indicated globally disseminated carbonate as a constituent of Martian dust [7]. TES spectra have shown the widespread occurrence of high-silica materials [8] thought to be related to aqueous alteration at high latitudes [9-12]. In addition, TES data have indicated that silicate alteration products may occur at low-but-significant levels at low latitudes [12], where variable olivine detection might be a sign of weathered regolith [13].

NIR data from OMEGA and CRISM and MIR data from TES and THEMIS are complementary. The NIR and MIR datasets seem, thus far, to afford generally consistent interpretations, though neither dataset is fully capable of observing what is seen in the other, owing to differences in what is measured between NIR and MIR wavelengths and how those spectral regions are affected by the physical and mineralogical conditions on the ground. It is necessary to employ both spectral regions to achieve a robust picture of Mars' alteration.

Studying weathering in the MIR: The MIR offers particular challenges to investigating chemical weathering, but with these challenges come great possibilities as well. MIR fundamentally measures lattice vibrations and can be used to detect important silicate minerals not seen in NIR, most notably feldspars. Differences in remotely sensed igneous mineral assemblages may result from aqueous weathering, and MIR data are uniquely suited to investigate weathering by seeking out mineralogical variations in primary silicate phases. Additionally, MIR data are sensitive to silicate alteration minerals that can go undetected in NIR, for instance in rock weathering rinds and silica rock coatings [14,15]. Consequently, MIR data provide a unique and robust means of investigating aqueous alteration.

Among the challenges, MIR observations of rocks and sand are adversely affected by dust deposition, temperature variations within a scene, and the cold temperatures often encountered on Mars. Yet the most significant challenge to chemical weathering studies in MIR is related to its strength—the vast majority of minerals that one attempts to measure are silicates. The technique of spectral unmixing (linear deconvolution) has enabled investigators to identify different minerals mixed at the sub-pixel scale, resulting in reliable, quantitative mineral identification for igneous and metamorphic rocks as well as coarse mineral mixtures [16-18]. Linear deconvolution techniques, however, break down for weathered surfaces because they tend to be (partly) fine-grained and coated surfaces in which emitted photons are scattered and interact with multiple mineral grains [15]; (An assumption of linear mixture models is that each photon has had a single mineral interaction). In addition, the products of weathering—often poorly-crystalline gels that have not been spectrally characterized—are unavailable to spectral libraries used in linear modeling [14,15]; (The other tenant of linear deconvolution is that each mineral in an observed surface is available in the spectral library). Thus, linear deconvolution should be avoided for weathered surfaces because it produces at least partially inaccurate results. And, whereas the strength of MIR spectroscopy is that it detects all silicates, the complications of modeling make it difficult to evaluate primary igneous minerals and secondary weathering phases alike. Therefore, a different technique is needed to evaluate weathered surfaces in the MIR.

Spectral indexing has been successfully used to identify dust cover and olivine and map their distributions on Mars [19,20]. Given the difficulties of performing linear deconvolution on weathered materials, spectral indices may provide a more robust, and more accurate, way to study weathering in the MIR.

Naturally weathered rocks in MIR: We collected weathered basaltic rocks from several arid to temperate environments, including the Columbia River Plateau in Washington state, Kohala volcano and Mauna Loa volcano in Hawaii, Tasmania, Victoria and New South Wales, Australia, and central Arizona. We collected 120 MIR emissivity spectra for naturally weathered surfaces and 77 spectra of fresh (cut and unweathered interior) surfaces for 77 different rock specimens. The 197 spectra were examined for spectral trends that distinguish fresh and weathered surfaces.

Weathering-related spectral indices: Compared to their corresponding fresh-rock spectra, the spectra of weathered surfaces tend to have lower emissivity in the 800-1000 cm^{-1} region, producing an overall V-shape in the Si-O-Si stretching region from 800-1200 cm^{-1} (Fig. 1). This shape, including a local emissivity maximum near 950 cm^{-1}, results from silicate weathering products in the weathering rinds that scatter and partly

mask photons emitted from the rock-forming minerals while they emit energy themselves. Between 380-400 cm^{-1}, spectra of fresh surfaces have an absorption feature related to plagioclase feldspar. That feature generally disappears in weathered surfaces, indicating either that plagioclase has been weathered out of the weathering rinds or, more likely, that it has been masked by weathering products. In addition, an O-Si-O bending feature common to weathering products appears in weathered samples at ~465 cm^{-1} (Fig. 1).

From these observations, we used two indices to differentiate fresh and weathered surfaces. The indices were normalized by dividing through with local emissivity minima to account for wide differences in spectral contrast. A 950-cm^{-1} index accounted for the reduced emissivity between 800-1000 cm^{-1} in weathered surfaces:

$$(\varepsilon_{950} - \varepsilon_{min}) / (1 - \varepsilon_{min(800\text{-}1200)}) \quad (1)$$

A 385-cm^{-1} index accounts for the loss of the absorption at 380-400 cm^{-1} and deeper 465 cm^{-1} feature in weathered samples:

$$1 + [(\varepsilon_{465} - \varepsilon_{385}) / (1 - \varepsilon_{465})] \quad (2)$$

When applied to spectral data of weathered basalts, the 385-cm^{-1} and 950-cm^{-1} features show appreciable scatter, but there is a distinctive trend (Fig. 2). Weathered surfaces are readily distinguished from fresh surfaces when viewed as averages of spectra from each sample locality. Weathered surfaces decrease in the 385-cm^{-1} index and increase in the 950-cm^{-1} index.

Comparison to Mars data: Applied to the TES-derived Surface Type 1 (ST1) and Surface Type 2 (ST2) spectra [14], the weathering indices indicate that ST2 is consistent with being a weathered version of ST1 (Fig 2); however, the magnitude of the difference may indicate that weathering of ST2 has been light relative to the terrestrial examples. Further work is needed to test these indices against TES data, and additional work is needed to determine the usefulness of spectral indices for evaluating chemical weathering.

References: [1] Bibring J.-P. et al. (2006) *Science*, *312*, 400-404. [2] Mustard J. F. et al. (2008) *Nature*, *454*, 305-309. [3] Bishop J. L. et al. (2008) *Science*, *321*, 830-833. [4] Gendrin A. et al. (2005) *Science*, *307*, 1587-1591. [5] Milliken R. E. et al., (2008) *Geology*, *36*, 847-850. [6] Ehlmann B. L. et al. (2008) Science, 322, 1828-1832. [7] Bandfield J. L. et al. (2003) *Science*, *301*, 1084-1087. [8] Bandfield J. L. et al. (2000) *Science*, *287*, 1626-1630. [9] Wyatt M. B. and McSween H. Y., Jr. (2002) *Nature*, *417*, 263-266. [10] Kraft M. D. et al. (2003) *GRL*, *30*, 2288. [11] Michalski J. R. et al. (2005) *Icarus*, *174*, 161-177. [12] Rogers A. D. and Christensen P. R. (2007) *JGR*, *112*, E01003. [13] Bandfield J. L. and Rogers A. D. (2008) *Geology*, *36*, 579-582. [14] Michalski J. R. et al. (2006) *EPSL*, *248*, 822-829. [15] Kraft M. D. et al. (2007) *AGU*, *88*, Fall Meet. Suppl., Abstract P13E-03. [16] Ramsey M. S. and Christensen P. R. (1998) JGR, 103, 577-596. [17] Feeley K. C. and Christensen P. R. (1999) *JGR*, *104*, 24195-24210. [18] Wyatt M. B. et al. (2001) JGR, 106, 14711-14732. [19] Ruff, S. W. and Christensen P. R. (2002) *JGR*, *107*, 5127. [20] Ruff S. W. and Christensen P. R. (2007), *GRL*, *34*, L10204.

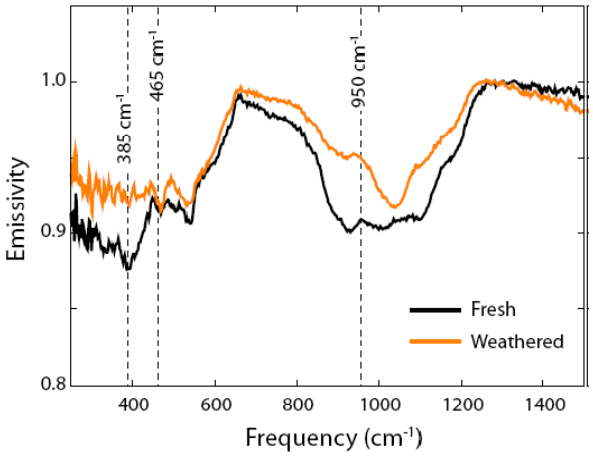

Figure 1. Example emissivity spectra of fresh and weathered basalt for sample GIL-06-04 from Gillespie Volcano, Arizona showing locations of parameters used in weathering indices.

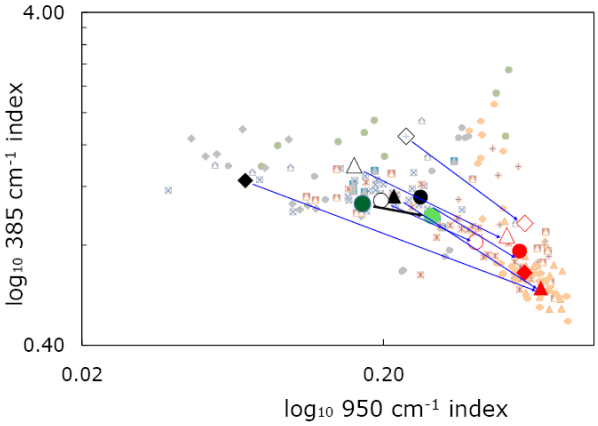

Figure 2. Plot of the 385-cm^{-1} index vs. the 950-cm^{-1} index for 197 spectra of fresh (grey symbols) and weathered (oragne symbols). Different symbol shapes and shading indicate samples from different localities. Averages for each location are plotted as black (fresh) and red (weathered) symbols. Lines tie the fresh and weathered averages for each location. ST1 (green circle) and ST2 (light green circle) are plotted for comparison to the trends in the terrestrial data.